



## Research article

# Assessing the impact of packaging materials on anoxic biotrickling filtration of siloxanes in biogas: Effectiveness of activated carbon in removal performance

Celia Pascual<sup>a,b</sup>, David Antolín<sup>a,b</sup>, Sara Cantera<sup>a,b</sup>, Raúl Muñoz<sup>a,b</sup>, Raquel Lebrero<sup>a,b,\*</sup>

<sup>a</sup> Department of Chemical Engineering and Environmental Technology, University of Valladolid, Dr. Mergelina s/n., Valladolid, 47011, Spain

<sup>b</sup> Institute of Sustainable Processes, University of Valladolid, Dr. Mergelina s/n., Valladolid, 47011, Spain



## ARTICLE INFO

## Keywords:

Activated carbon  
Biogas upgrading  
Biotrickling filter  
Nanoparticles  
Siloxanes anoxic removal

## ABSTRACT

Siloxanes (VMS) represent a class of organosilicon compounds known for their adverse effects on both the environment and human health. Their presence in biogas significantly hinders its economic valorisation, highlighting the need for effective treatment methods. This study investigates the performance of three different packing materials in the anoxic biofiltration of VMS (L2, L3, D4 and D5). The materials evaluated included plastic rings (BTF-1), polyurethane foam (BTF-2) and plastic rings combined with activated carbon (80:20) (BTF-3). Among them, BTF-3 exhibited superior performance, achieving maximum VMS removal efficiencies (REs) of 90%, including the complete elimination of L3 and D4, and ~80% removal of D5, attributed to the presence of activated carbon. However, the abatement of L2 was inferior to that of other VMS (<80%), which was attributed to the activated carbon's affinity for larger molecular weights and critical diameters. In contrast, BTF-1 and BTF-2 supported maximum VMS removals of 40%. Notably, neither increasing the trickling liquid velocity from 2 to 4.5 m h<sup>-1</sup> nor adding Fe-carbon nanoparticles to the solution had any impact on the BTFs' performance. Following the successful results observed in BTF-3, gas residence time was reduced from 60 to 42 min, consequently leading to an increase in the EC from 366 to 509 mg m<sup>-3</sup> h<sup>-1</sup> (corresponding to an RE = 87%). Despite the different performance of the BTFs, comparable bacterial communities were identified, dominated by the genera *Thermomonas*, *Corynebacterium*, *Aquimonas*, *Thauera* and *Parvibaculum*. The results obtained in this study highlighted the potential of activated carbon as packing material for enhancing abatement performance during biotrickling filtration and identified new bacterial genera with potential for VMS degradation.

## 1. Introduction

Siloxanes, also referred to as silicones, are organosilicon compounds widely utilized in industrial applications due to their exceptional properties. Their molecular structure consists of -Si-O- chains with two methyl groups (-SiMe<sub>2</sub>-O-) linked to the silicon atoms. Short-chain and low molecular weight siloxanes are identified as volatile methyl siloxanes (VMS). Their extensive commercial use results in gas emissions into the atmosphere, raising environmental concerns regarding bioaccumulation and toxicity (Alton and Browne, 2021; Pascual et al., 2021a). Moreover, their presence in biogas triggers detrimental infrastructure effects during its combustion, as the oxidation of VMS produces SiO<sub>2</sub> particles that physically damage engines and turbines (Alves

et al., 2023; de Arespacochaga et al., 2020). To address this issue, a regulatory concentration limit of 10 mg siloxanes m<sup>-3</sup> has been established for the utilization of biogas as a vehicle fuel or its injection into the natural gas grid within the European Union framework (Standardization, 2018). This underscores the critical importance of eliminating VMS, especially in the context of biogas purification and utilization, aligning with the goal of the European Green Deal to decarbonise the EU energy system (<https://www.consilium.europa.eu/en/policies/green-deal/>).

To eliminate these compounds from gaseous emissions, multiple technologies have been successfully developed, with physical-chemical processes emerging as the most common and effective solutions. Among them, adsorption on conventional materials such as activated

\* Corresponding author. Department of Chemical Engineering and Environmental Technology, University of Valladolid, Dr. Mergelina s/n., Valladolid 47011, Spain.

E-mail address: [raquel.lebrero@uva.es](mailto:raquel.lebrero@uva.es) (R. Lebrero).

<https://doi.org/10.1016/j.jenvman.2024.122862>

Received 9 July 2024; Received in revised form 4 October 2024; Accepted 7 October 2024

Available online 14 October 2024

0301-4797/© 2024 The Authors. Published by Elsevier Ltd. This is an open access article under the CC BY license (<http://creativecommons.org/licenses/by/4.0/>).

carbon or silica gel stand out as the most commonly implemented at industrial scale (Gaj, 2020; Rivera-Montenegro et al., 2023; Shen et al., 2018). Recent research in this field has focused on new pathways to improve the performance of these processes. The surface modification of activated carbon or metal oxides has been proven to be a successful method for increasing the adsorption capacity of VMS, as the hydrophobicity of the adsorbent surface is reduced (Lv et al., 2023a, 2023b). However, the search for environmentally sustainable alternatives to reduce the high carbon footprint and operational costs of physical-chemical technologies has directed recent research efforts toward biological processes, known for their minimal environmental impact. In this context, biotrickling filters (BTF) are the most implemented and best-performing configuration for treating low and variable pollutant concentration gaseous streams (Sakhaei et al., 2023; Urban et al., 2009).

The main drawback of BTFs as a VMS-abatement solution is the limited mass transfer of these compounds to the aqueous nutrient solution sustaining microbial activity (high dimensionless Henry's law solubility constant (Equation (1)); L2: 404, L3: 1440, D3: 72, D4: 252; D5: 183 ([www.henry-law.org](http://www.henry-law.org))).

$$H_{G/L} = \frac{C_G}{C_L^*} \quad \text{Equation 1}$$

where  $C_L^*$  represent the gaseous compound concentration in the interphase in equilibrium with the compound concentration in the gas phase ( $C_G$ ).

The high hydrophobicity of VMS results in low removal efficiencies, typically ranging from 20 to 50% in conventional BTFs (Accettola et al., 2008; Pascual et al., 2020; Popat and Deshusses, 2008). To overcome this limitation, different mass transfer strategies have been explored in this field over the last decade. Li et al. (2014) were pioneers in assessing the removal of octamethylcyclotetrasiloxane (D4) by *Pseudomonas aeruginosa*, a species that segregates biosurfactants. These substances enhance the solubility of hydrophobic pollutants, thereby increasing their bioavailability and promoting their microbial degradation. The presence of biosurfactants can lead to a significant increase in the removal efficiency (RE) of D4 up to 74% (Li et al., 2014). Based on this finding, two-phase partitioning BTFs (TP-BTFs) have been successfully applied for the efficient removal of VMS. In a TP-BTF, an organic solvent with high affinity for the hydrophobic gas pollutants is added to the aqueous media, enhancing both their gas-liquid mass transfer and subsequent biodegradation. Previous investigations have reported REs of up to 90% for cyclic VMS (D4 and decamethylcyclopentasiloxane-D5) in a TP-BTF packed with plastic rings, operating with a gas empty bed residence time (EBRT) of 60 min and an inlet concentration of around 200 mg m<sup>-3</sup> for each compound (Pascual et al., 2020, 2021b). However, this configuration exhibited inferior performance in removing linear VMS (hexamethyldisiloxane-L2 and octamethyltrisiloxane-L3), with their removal efficiencies ranging between 20 and 50% for inlet concentrations of approximately 200 mg m<sup>-3</sup>.

The choice of packing material can also play a crucial role in the performance of BTFs. Plastic rings, lava rock, and ceramic rings are commonly used as packing materials for VMS removal (Accettola et al., 2008; Li et al., 2014; Pascual et al., 2022a; Popat and Deshusses, 2008). Nevertheless, there are few studies in literature that comparatively examine the influence of various materials as packed beds for VMS removal. Polyurethane foam, a material with excellent properties (high superficial area, resistant to attack from organic solvents and microbes, ease of handling and good regeneration ability) has been successfully employed for the removal of different volatile organic compounds such as toluene, ethylbenzene, hydrogen sulphide or ammonia (Pérez et al., 2016; Rybarczyk et al., 2019). Similarly, porous activated carbon (AC) has been employed in optimizing anoxic biofiltration of sulphur compounds due to its exceptional capacity for adsorbing nutrients, pollutants, and biomass (Duan et al., 2006, 2005; Korotta-gamage and

Sathasivan, 2017; Lebrero et al., 2014). The selected packing material should provide an appropriate structure for microbial growth and high porosity to facilitate optimal gas circulation through the bed. The combination of different materials can be an effective choice to enhance the performance of the packed bed (Urbaniec et al., 2020). For instance, Santos-Clotas et al. (2019a) operated a BTF packed with lava rock and a thin layer of activated carbon at the top of the bed for the simultaneous removal of VMS (D4 and D5), toluene, limonene and hexane. The combination of these packing materials led to a significant increase in VMS removal compared to previous stages without activated carbon. This improvement was attributed to both the alleviation of mass transfer limitations due to the presence of activated carbon and the efficient biomass growth facilitated by the material, which supports effective cell attachment and ensures an adequate electron acceptor availability (Santos-Clotas et al., 2019a). An alternative configuration for packed bed reactors in VOC treatment involves mixing different packing materials throughout the bed, rather than layering them (Sun et al., 2012). Given the adsorptive properties of activated carbon, which enhance the transport of hydrophobic pollutants from the gas phase to the biofilm, its even distribution in the BTF could significantly improve the mass transfer across the entire packed bed, rather than being confined to a localized layer. Additionally, the incorporation of nanoparticles (NPs) in a bioreactor has been explored to enhance the mass transfer of both VOCs and hydrophobic compounds. NPs promote mass transfer and biomass growth due to their high adsorption capacity, large surface area to volume ratio and abundant active sites (Vargas-Estrada et al., 2023). However, both strategies have not yet been applied to the removal of VMS, and this study constitutes the first proof of concept of their impact on linear siloxanes. Therefore, a novel and potential study pathway is opening to improve the mass transfer of siloxanes in BTFs.

In this study, the biodegradation capacity of three BTFs constructed with different packing materials for the removal of key VMS typically found in biogas (L2, L3, D4 and D5) was evaluated under anoxic conditions. The evaluated packing materials were plastic rings, polyurethane foam and a mixture of plastic rings and activated carbon (80:20 v/v) distributed throughout the entire bed. The effect of the addition of mesoporous iron and carbon based NPs to the trickling solution was also assessed. To gain insights into the operational parameters of the process, variations in the EBRT and the trickling liquid velocity were also investigated.

## 2. Materials and methods

### 2.1. Mineral salt medium and inoculum preparation

The mineral salt medium (MSM) was composed of (g L<sup>-1</sup>): KH<sub>2</sub>PO<sub>4</sub>, 0.7; K<sub>2</sub>HPO<sub>4</sub>·3H<sub>2</sub>O, 0.917; KNO<sub>3</sub>, 3; NaCl, 0.2; MgSO<sub>4</sub>·7H<sub>2</sub>O, 0.345; CaCl<sub>2</sub>·2H<sub>2</sub>O, 0.026; and 2 mL L<sup>-1</sup> of a micronutrient solution containing (g L<sup>-1</sup>): EDTA, 0.5; FeSO<sub>4</sub>·7H<sub>2</sub>O, 0.2; ZnSO<sub>4</sub>·7H<sub>2</sub>O, 0.01; MnCl<sub>2</sub>·4H<sub>2</sub>O, 0.003; H<sub>3</sub>BO<sub>3</sub>, 0.003; CoCl<sub>2</sub>·6H<sub>2</sub>O, 0.02; CuCl<sub>2</sub>·2H<sub>2</sub>O, 0.001; NiCl<sub>2</sub>·6H<sub>2</sub>O, 0.002; NaMoO<sub>4</sub>·2H<sub>2</sub>O, 0.003 (Pascual et al., 2023). All chemicals used for the preparation of the MSM were purchased from Panreac (Barcelona, Spain). L2 (98.5% purity), L3 (98% purity), D4 (98% purity) and D5 (97% purity) were obtained from Sigma Aldrich (San Luis, USA).

The BTFs were inoculated with activated sludge from the wastewater treatment plant of Valladolid (Spain). Prior inoculation, the microbial community was acclimated to VMS for 31 days in two 2-L bottles. For this purpose, 900 mL of the fresh sludge were centrifuged for 10 min at 10,000 rpm and the pellet was resuspended in 450 mL of fresh mineral medium. The bottles headspace was flushed with N<sub>2</sub> 5.0 (Abello Linde Spain, purity >99.9%) prior supplementation of 20 mL of a gas mixture containing VMS (L2, L3, D4 and D5), equivalent to an individual concentration of ~50 mg m<sup>-3</sup> for each compound. This concentration was used to acclimate the culture to the operating conditions of the BTFs, which are similar to those typically found in biogas. By day 31, the

acclimated sludge from both bottles was mixed and an aliquot of 450 mL was employed as inoculum for the BTFs. The remaining sludge was returned to a single bottle where the headspace and liquid phase were replaced according to the inoculum preparation procedure. The culture was maintained under acclimatisation until day 71, when it was used to reinoculate the BTFs.

## 2.2. Experimental set up

The experimental setup (Fig. 1) consisted of three 2-L cylindrical PVC columns (8.4 cm diameter, 37.5 cm height) packed with different packing materials: Kaldnes K1 Micro rings (7 mm diameter, 9 mm length, specific surface area:  $950 \text{ m}^2 \text{ m}^{-3}$ , density:  $197 \text{ g L}^{-1}$ , BTF-1), polyurethane foam (foam blocks custom-cut for the column, specific surface area of  $1000 \text{ m}^2 \text{ m}^{-3}$ , density:  $22 \text{ g L}^{-1}$ , BTF-2) and a mixture of activated carbon (particle size: 0.5–3.15 mm, density:  $450 \text{ g L}^{-1}$ ) and Kaldnes K1 Micro rings at a ratio of 20:80 v/v (BTF-3). The inlet VMS-loaded stream was prepared by injecting a mixture of four different siloxanes (L2, L3, D4 and D5) with a syringe pump (Fusion 100, Chemyx Inc. USA) into a  $\text{N}_2$  stream. The synthetic stream was directed through two 1 L mixing chambers to ensure complete homogenization of the VMS. The homogenized stream was divided into three separate streams, each flowing at a rate of  $33 \text{ mL min}^{-1}$ . These individual streams were precisely controlled using three single rotameters and introduced at the bottom of each biotrickling filter (BTF). The MSM, continuously irrigated to each BTF, was stored in a 1-L nutrient reservoir connected to the column and equipped with a magnetic plate. From the reservoir, the MSM was continuously recycled to the top of each column countercurrently with the VMS-loaded  $\text{N}_2$  stream.

Prior to inoculation, a 15-day abiotic test was conducted in the BTFs to confirm the absence of any VMS physical-chemical abatement. The test was initially developed with the empty PVC columns, then with the columns filled with the packing materials and finally with the recycling liquid solution trickling over the beds. This sequential approach ensured that any observed changes or effects could be attributed specifically to biodegradation, eliminating potential physical-chemical interactions within the system.

The system was continuously operated for 126 days in different experimental periods (Table 1). During the first 79 days, the three BTFs were operated at an EBRT of 60 min and a trickling liquid velocity (TLV) of  $2 \text{ m h}^{-1}$  (Stage I), as these conditions were found optimal in previous research (Pascual et al., 2021b). By day 80 onwards, the EBRT in BTF-3 was reduced to 42 min to optimize the operating conditions and reduced

investment costs, while the TLV was increased to  $4.5 \text{ m h}^{-1}$  in BTF-1 and BTF-2 (Stage II) to enhance VMS mass transfer. Finally, the addition of carbon coated zero valent iron NPs containing 7.26 % (wt%) of iron (CALPECH NPs) to the trickling liquid solution was implemented in the three BTFs by day 110 (Stage III). For this purpose, 1 g of NPs was resuspended in 100 mL of trickling liquid solution and returned to the nutrient reservoir of each BTF. During the entire experiment, a weekly replacement of 300 mL of the trickling liquid solution with fresh MSM was carried out, equivalent to a hydraulic retention time of 47 days. Analysis of the withdrawn cultivation broth included measurements of pH, total organic carbon (TOC), inorganic carbon (IC), total nitrogen (TN), nitrite and nitrate concentrations. The inlet and outlet VMS concentrations in the gas streams and the pressure drop across the packed beds were periodically analysed.

## 2.3. Analytical procedures

The analysis of VMS concentration in the gas phase at the inlet and outlet of the BTFs was performed using an Agilent 8860 gas chromatograph (Santa Clara, California, USA) equipped with a flame ionization detector (FID) and a HP-5 column (15 m  $\times$  0.25 mm  $\times$  0.25  $\mu\text{m}$ ). Both the detector and injector temperatures were maintained constant at  $250 \text{ }^\circ\text{C}$ . The oven temperature was initially set at  $40 \text{ }^\circ\text{C}$  for 2.0 min and then increased at  $30 \text{ }^\circ\text{C min}^{-1}$  to  $180 \text{ }^\circ\text{C}$ , maintained for 1 min, and increased again at  $30 \text{ }^\circ\text{C min}^{-1}$  to  $200 \text{ }^\circ\text{C}$ . Helium was used as the carrier gas at a flow rate of  $3.5 \text{ mL min}^{-1}$ .

For the daily determination of  $\text{CO}_2$  and  $\text{O}_2$  gas concentrations, a Bruker 430 gas chromatograph (Palo Alto, USA) coupled with a thermal conductivity detector and equipped with a CP-Molsieve 5A (15 m  $\times$  0.53 mm  $\times$  15  $\mu\text{m}$ ) and a P-PoraBOND Q (25 m  $\times$  0.53 mm  $\times$  10  $\mu\text{m}$ ) columns was used. Oven, detector and injector temperatures were maintained constant at 45, 200 and  $150 \text{ }^\circ\text{C}$  for 5 min, respectively. Helium was used as the carrier gas at a flow of  $13.7 \text{ mL min}^{-1}$ .

The total organic carbon (TOC), total inorganic carbon (IC), total nitrogen (TN), nitrite and nitrate concentrations in the cultivation broth were periodically analysed. TOC, IC and TN concentrations were measured using a TOC-VCSH analyser coupled with a TNM-1 chemiluminescence module (Shimadzu, Japan). Finally, nitrite and nitrate were determined in a HPLC-IC using a Waters 515 HPLC pump coupled with a conductivity detector (Waters 432) and equipped with an IC-Pak Anion HC column (4.6  $\times$  150 mm) and an IC-Pak Anion Guard-Pak (Waters).

The average values of the data and results presented in the

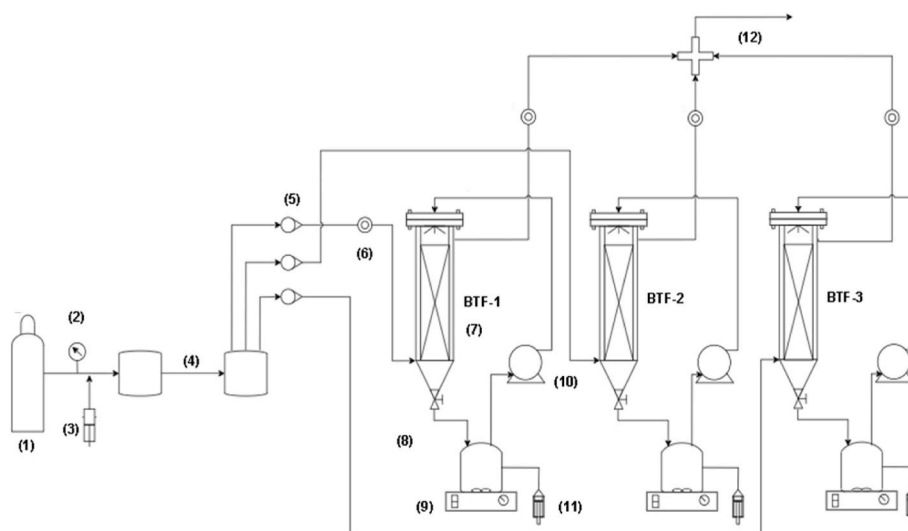


Fig. 1. Experimental setup representation: (1)  $\text{N}_2$  cylinder, (2) pressure gauge, (3) syringe pump, (4) mixing chambers, (5) rotameters, (6) gas sampling ports, (7) BTFs, (8) mineral medium reservoir, (9) magnetic stirrer plate, (10) peristaltic pumps, (11) liquid sampling ports, (12) outlet gas stream.

**Table 1**  
Experimental conditions tested in the BTFs.

Stage	Elapsed time (days)	Inlet VMS concentration (mg m <sup>-3</sup> )	EBRT (min)			Trickling liquid velocity (TLV) (m h <sup>-1</sup> )			Nanoparticles (NPs)		
			BTF-1	BTF-2	BTF-3	BTF-1	BTF-2	BTF-3	BTF 1	BTF-2	BTF-3
I	0–79	251 ± 63	60	60	60	2	2	2	–	–	–
II	80–109	327 ± 57	60	60	42	4.5	4.5	2	–	–	–
III	110–126	297 ± 61	60	60	42	4.5	4.5	2	Addition of 1 g of carbon coated zero valent iron NPs to the trickling liquid solution.		

manuscript were calculated using the arithmetic mean and standard deviation.

#### 2.4. Bacterial community analysis

Samples of 20 mL of the biofilm of the three BTFs were withdrawn at the end of the operation for prokaryotic population analysis. The DNA was extracted from each biological replicate with a FastDNA™ SPIN Kit for Soil (MP Biomedicals, USA). PCR amplification of regions 16S-V4-V5 was performed using the primers GTGCCAGCMGCCGCGGTAA, CCGTCAATTCCTTTGAGTTT connecting with barcodes. Libraries were quality checked with Qubit and real-time PCR for quantification, while a bioanalyzer was used for size distribution detection. Quantified libraries were pooled and sequenced on a paired-end Illumina platform to generate 250bp paired-end raw reads in Novogene UK (Cambridge, UK). Paired-end reads were assigned to samples based on their unique barcodes and truncated by cutting off the barcodes and primer sequences. Bioinformatic further analysis was performed with Python (V3.6.13). Paired-end reads were merged using FLASH (V1.2.11, <http://ccb.jhu.edu/software/FLASH/>) (Magoc and Salzberg, 2011). Data filtration and chimera removal were performed using the fastp (V0.23.1) software and the UCHIME Algorithm ([http://www.drive5.com/usearch/manu al/uchime\\_algo.html](http://www.drive5.com/usearch/manu al/uchime_algo.html)) (Edgar et al., 2011). Clustering of the sequences into Operational Taxonomic Units (OTUs) was based on the gene reference database SILVA (V138.1) and the ribosomal data base project (V18) (Quast et al., 2013) using QIIME (V 1.9.1). The sequences obtained have been deposited in Genbank as Bioproject: PRJNA1062140. Bar graph was plotted with R using the package ggplot2 (Wickham, 2009). The differences between samples regarding microbial community structures were calculated via dimension reduction. T-test were used to calculate the significance of the structure of microbial community differences between samples.

### 3. Results and discussion

#### 3.1. Abiotic test

During the first stage of the abiotic test (empty PVC columns), no significant differences were observed between the inlet and outlet concentrations of the target VMS. This observation indicated the absence of physical-chemical adsorption (Fig. S1). The outlet concentration initially decreased below the inlet concentration upon starting the trickling liquid and introducing the packing media into BTF-2 and BTF-3. However, as the packing material and trickling solution became saturated, an increase in the outlet concentration was recorded. In BTF-1, no adsorption or absorption of VMS was recorded, as both the inlet and outlet concentrations remained consistently similar throughout the entire test. Additionally, no CO<sub>2</sub> production was detected during the abiotic experiment, confirming a lack of biological activity.

#### 3.2. Influence of the packing media on VMS abatement

As a results of the presence of activated carbon, higher anoxic removals were observed in BTF-3 compared to BTF-1 and BTF-2, which showed similar results for all VMS.

#### 3.2.1. Stage I: Role of activated carbon

BTF-3 exhibited a superior performance for all the compounds throughout the entire experiment. The total removal of VMS (Fig. 2) was approximately 2 times higher compared to that recorded in BTF-1 and 1.6 times higher than in BTF-2, with an average steady value of 90.3 ± 3.5% during the initial days of Stage I (corresponding to an elimination capacity (EC) of 366 ± 7 mg m<sup>-3</sup> h<sup>-1</sup>). L2 was completely removed in BTF-3 within the first days of the experiment (Fig. 3). However, the removal slightly decreased to 84.9 ± 4.5% between days 43 and 56. This reduction was associated with: (i) initial adsorption on activated carbon until reaching the breakthrough point and the equilibrium adsorption-biodegradation (Santos-Clotas et al., 2019a) and (ii) the decrease in L2 inlet concentration from ~60 to ~30 mg m<sup>-3</sup> (Fig. S2). According to the volumetric pollutant mass transfer rate equation (Equation. (2)), this decrease in the inlet concentration resulted in a reduction of the concentration gradient and, consequently, the global mass transfer coefficient (Pascual et al., 2022a)

$$F_{G/L} = K_{G/L}^a \left( \frac{C_G}{H_{G/L}} - C_L \right) \quad \text{Equation 2}$$

where  $F_{G/L}$  represents the volumetric mass transfer rate (g m<sup>-3</sup> h<sup>-1</sup>),  $K_{G/L}^a$  is the overall volumetric mass transfer coefficient (h<sup>-1</sup>),  $C_G$  and  $C_L$  are the compound concentrations (g m<sup>-3</sup>) in the gas and liquid phase, respectively, and  $H_{G/L}$  the dimensionless Henry's law constant for the gaseous compound (Equation (1)).

In contrast, L3 RE fluctuated between 60 and 100% during the initial days of the experiment, stabilizing at 100% by day 34 despite the inlet concentration decreased from ~70 to ~45 mg m<sup>-3</sup>. Likewise, the RE for both D4 and D5 initially fluctuated around 80%. However, while the RE for D5 remained consistent throughout the rest of experiment at an average value of 81.9 ± 6.8%, it stabilized at 100% for D4 by day 42.

In both BTF-1 and BTF-2, the total VMS removal remained around 40% at the beginning of Stage I. However, this value decreased to 21.7 ± 11.8 in BTF-1 and 14.7 ± 6.1% in BTF-2 between days 46 and 56. As previously discussed, this decrease was associated with the lower inlet concentration of D4 and D5, leading to a reduction in the overall VMS inlet concentration (Fig. S3) and, consequently, in the global mass transport of VMS. In this sense, D5 RE values remained at 73.7 ± 8.5 and 76.5 ± 12.5% in BTF-1 and BTF-2, respectively, at the beginning of Stage I, followed by a progressive decrease between days 42 and 56, stabilizing at 24.6 ± 11.2% in BTF-1 and 25.6 ± 11.1 % in BTF-2. Interestingly, distinct performance was observed for D4 during the start-up of each BTF. In BTF-1, no removal of D4 was recorded until day 11, reaching a maximum of 39.3% by day 32. In BTF-2, D4 immediately achieved a RE of 46%, which gradually decreased and stabilized around 20% up to day 56. For linear VMS, significant removal was not observed in either BTF-1 or BTF-2 until day 17. Subsequently, the RE increased and remained between 20 and 40% before declining below 25% between days 42 and 56.

The instability observed in BTF-1 and 2 was attributed to fluctuations in the inlet concentrations of VMS. Conversely, BTF-3 exhibited greater robustness attributed to the activated carbon, which acted as a VMS reservoir during both low and high concentration periods. The superior performance of BTF-3 throughout the entire experiment confirmed the advantages provided by activated carbon as packing material compared

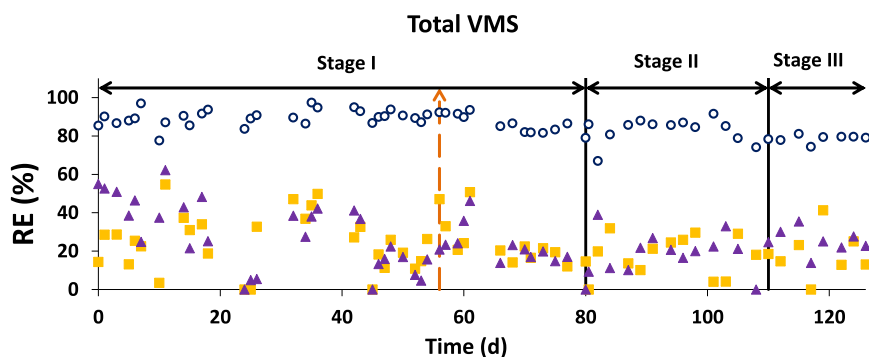


Fig. 2. Time course of total VMS removal efficiency in BTF-1(■), BTF-2(▲) and BTF-3(○) throughout the experiment. Vertical lines represent the different stages of the test: EBRT of 60 min and TLV of 2 m h<sup>-1</sup> (Stage I), reinoculation of the BTFs (----), increase of TLV to 4.5 m h<sup>-1</sup> in the BTF-1 and 2 and decrease of the EBRT to 42 min in the BTF-3 (Stage II) and addition of nanoparticles to the trickling solution (Stage III).

to plastic rings (BTF-1) and polyurethane foam (BTF-2). According to Santos-Clotas et al. (2019a), the adsorption of VMS on activated carbon likely avoided mass transfer limitations, facilitated efficient biomass growth through the material, and potentially promoted the ring-opening of cyclic VMS through the action of oxygen functional groups present on its surface (hydrolysis reactions), with their subsequent transformation into more soluble compounds (Santos-Clotas et al., 2019a). However, our study was unable to confirm this hypothesis due to the low siloxane load fed to the BTFs and the different nature of the packing materials. Consequently, the expected efficient biomass growth could not be verified through the pressure drop measurements, which remained consistently between 0.1 and 0.2 mbar in the three BTF throughout the experiment.

By day 56, the three BTFs were reinoculated with an enriched culture to stimulate the growth of the siloxanes degrading bacteria in the packed bed, aiming to enhance the performance of BTF-1 and BTF-2. In general, no significant differences were observed in BTF-3, where the total VMS removals remained at 87.2 ± 4%, corresponding to an EC of 326 ± 4 mg m<sup>-3</sup> h<sup>-1</sup> (Fig. 4). Until the end of this stage, a complete removal of L3 was achieved in BTF-3, with D4 maintaining a steady RE of 95.5 ± 1.0% and D5 experiencing a slight decrease in RE to 75.3 ± 5.3% (corresponding to EC values of 64 ± 5, 87 ± 4 and 137 ± 35 mg m<sup>-3</sup> h<sup>-1</sup>, respectively). However, the L2 removal performance in BTF-3 exhibited a progressive deterioration, reaching values of 56% (EC of 23 mg m<sup>-3</sup> h<sup>-1</sup>) by the end of Stage I, which was directly associated with competitive adsorption in the activated carbon as the available adsorption sites became saturated. In this sense, the lower adsorption capacity of different activated carbons for L2 compared to the rest of VMS has been previously reported (Tran et al., 2019). Consequently, the mass transfer enhancement related to the adsorption on activated carbon was lower in the case of L2 in BTF-3. Tran et al. (2019) also found that the adsorption capacity of activated carbon increased with longer chain lengths for linear VMS, whereas the opposite trend was observed for cyclic VMS. This fact could account for the lower performance obtained in the present work for D5 compared to D4.

In BTF-1 and BTF-2, VMS removal increased to 43–55% after reinoculation regardless of the compound, but decreased again to preceding values. Therefore, although the inoculation of the enriched culture initially boosted the growth of siloxanes-degrading bacteria and enhanced the removal performance of BTF-1 and 2, this overgrowth proved unsustainable throughout the remainder of the experiment.

### 3.2.2. Stage II: Reduction in the EBRT

The superior performance achieved in BTF-3 allowed a reduction in the EBRT from 60 to 42 min during Stage II, thus optimizing operational conditions. Notably, this reduction exerted no detrimental impact on the overall anoxic removal of the VMS, maintaining a consistent RE of 86.8 ± 2.8% (EC of 509 ± 56 mg m<sup>-3</sup> h<sup>-1</sup>) throughout this stage (Fig. 4). The

increase in the EC with the reduced EBRT indicated the absence of limitations associated to biological activity in BTF-3, suggesting that the system was primarily limited by mass transfer. This trend was observed for L3, D4, and D5, with average REs of 99.6 ± 0.8%, 97.0 ± 1.5%, and 86.9 ± 2.3%, respectively. While recent research showcased the remarkable performance of TP-BTF for VMS elimination operated at an EBRT of 60 min and at an inlet VMS concentration of 650 mg m<sup>-3</sup>, it is noteworthy that the removals achieved in those previous studies (80 % for L3 and 90% for D4 and D5) were comparatively lower than the ones obtained in the present study (Pascual et al., 2020). Moreover, in previously operated TP-BTFs, reducing the EBRT to 45 min resulted in a decline in the removal performance to values of 21, 58, 71 and 85% for L2, L3, D4, and D5, respectively, in contrast to the findings of this study (Pascual et al., 2021b). Consequently, the results obtained in the present study exceeded the highest achieved REs for L3, D4, and D5 observed in BTFs to date.

The removal efficiency of L2 exhibited fluctuations between 42 and 70%, progressively decreasing to 6.1% at the end of Stage II in BTF-3. The initial hypothesis of achieving complete L2 removal within the first 17 days of the experiment was based on the assumption of an initial adsorption onto the activated carbon followed by subsequent biodegradation. However, the continuous exposure of AC to siloxanes likely mediated the saturation of most adsorption sites, preferentially by other VMS such as L3, D4, and D5, along with the colonization of AC by bacterial growth on its surface. Overall, VMS with higher molecular weight and critical diameter such as L3, D4 and D5, preferentially adsorb over smaller VMS like L2, potentially hindering the adsorption on AC of the latter (Santos-Clotas et al., 2019b). This fact likely reduced the availability of L2 for the microbial community and explains the progressive decrease of the RE of L2 during the experiment and the superior performances achieved for L3, D4 over D5 in BTF-3.

In an attempt to improve the VMS removal performance of BTF-1 and BTF-2, the TLV was increased from 2 to 4.5 m h<sup>-1</sup> in these systems. Theoretically, a moderate increase in the TLV of a BTF promotes a more uniform distribution of the liquid throughout the packed bed, consequently enhancing the mass transfer coefficient and ultimately a more homogeneous growth of the biofilm in the packed bed. This positive effect has been previously reported in conventional BTFs designed for the removal of H<sub>2</sub>S, methane and other VOCs (Bu et al., 2021; Estrada et al., 2014), as well as in the removal of VMS in a TP-BTF (Pascual et al., 2023). In fact, Pascual et al. (2023) observed an increased RE for linear VMS when the TLV was raised from 2 to 10 m h<sup>-1</sup>. Despite this rational, no significant differences in the RE were observed in the present study compared to the previous stage, with total VMS removal values fluctuating around 20% during Stage II. Unlike in TP-BTFs, where an organic phase with a high affinity for the VMS is added, the trickling solution of both BTF-1 and 2 consisted of an aqueous solution. Thus, the enhancement of the distribution of the trickling solution on the packed bed

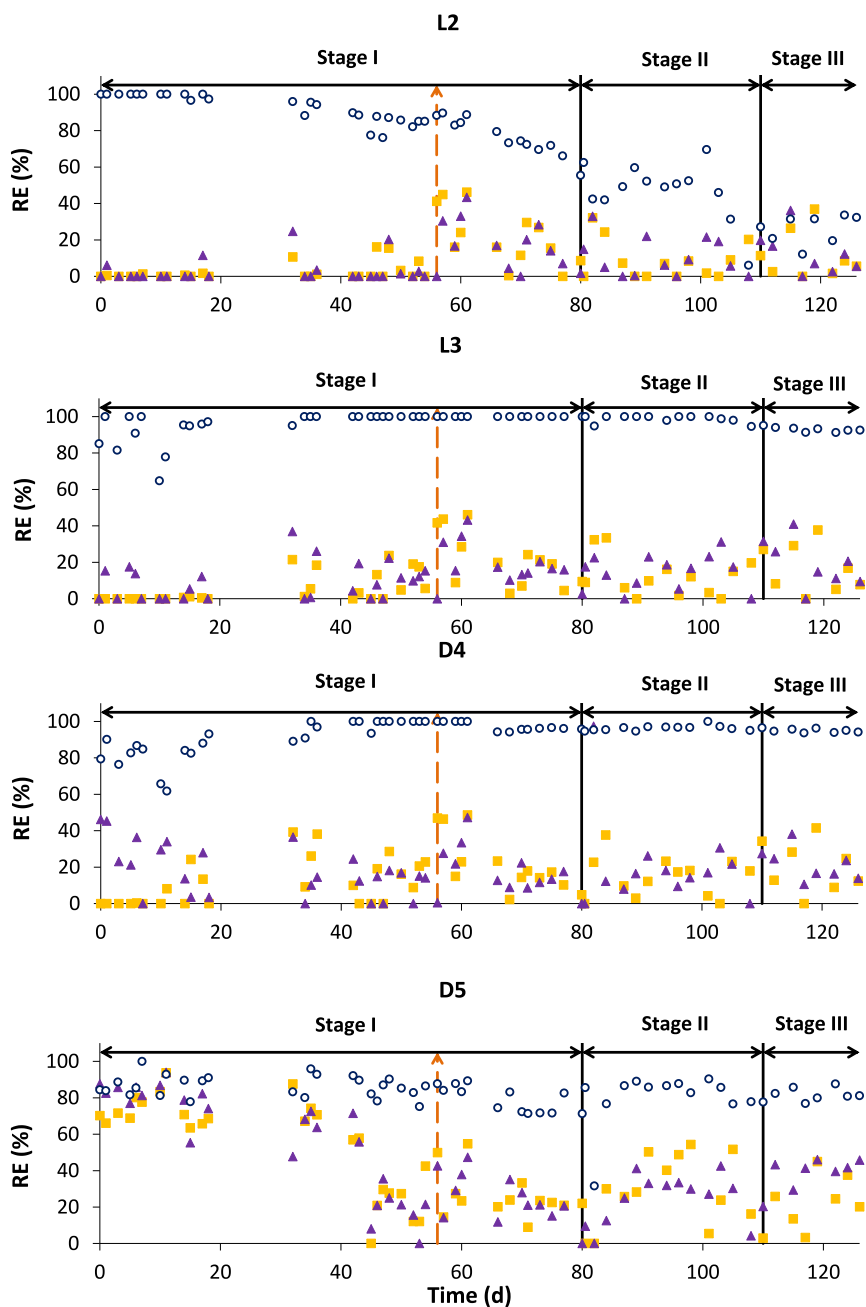


**Fig. 3.** Time course of L2, L3, D4 and D5 removal efficiency in BTF-1 (■), BTF-2 (▲) and BTF-3 (○). Vertical lines represent the different stages of the test: EBRT of 60 min and TLV of  $2 \text{ m h}^{-1}$  (Stage I), reinoculation of the BTFs (---), TLV increase to  $4.5 \text{ m h}^{-1}$  in BTF-1 and 2 and EBRT decrease to 42 min in BTF-3 (Stage II), and addition of nanoparticles to the trickling solution (Stage III).

exhibited no effect on the performance of both systems since the high hydrophobicity of VMS overrode the improvement of the mass transfer coefficient with the TLV.

### 3.2.3. Stage III: Effect of nanoparticles

By day 110, 1 g of Fe-carbon nanoparticles was added to the trickling solution of the three BTFs in order to improve the mass transfer of the VMS due to the low performance of BTF-1 and BTF-2. This strategy has been proven successful in bioreactors with suspended biomass, where the NPs enhance the transfer of gaseous pollutants to the biomass through hydrodynamic and shuttle effects. Specifically, Fe-carbon nanoparticles have shown promising results in improving the bioavailability of pollutants by increasing the surface contact between the gas phase and the active biomass (Kluytmans et al., 2003; Vargas-Estrada

et al., 2023). However, no positive effect was observed in the performance of the BTFs, remaining the total VMS RE at low values of  $18.6 \pm 12.0\%$  in BTF-1 and  $25.2 \pm 6.3\%$  in BTF-2 (Fig. 4). One possible explanation for this lack of improvement could be related to the specific interaction between the nanoparticles and the BTF media. Unlike systems with suspended biomass, where NPs can freely move and enhance pollutant diffusion, the presence of a packed bed in BTFs could have limited the gas-NP contact and therefore their effectiveness. Another possible reason could be that the nanoparticle dosage ratio was not optimized, and a higher amount might have been necessary to observe a positive effect. Moreover, a slight decrease in BTF-3 to  $78.7 \pm 2.0\%$  was observed which was likely attributed to the colonization of the adsorption sites of the activated carbon by NPs, leading to a subsequent decrease in the mass transfer rate, biomass growth efficiency and the

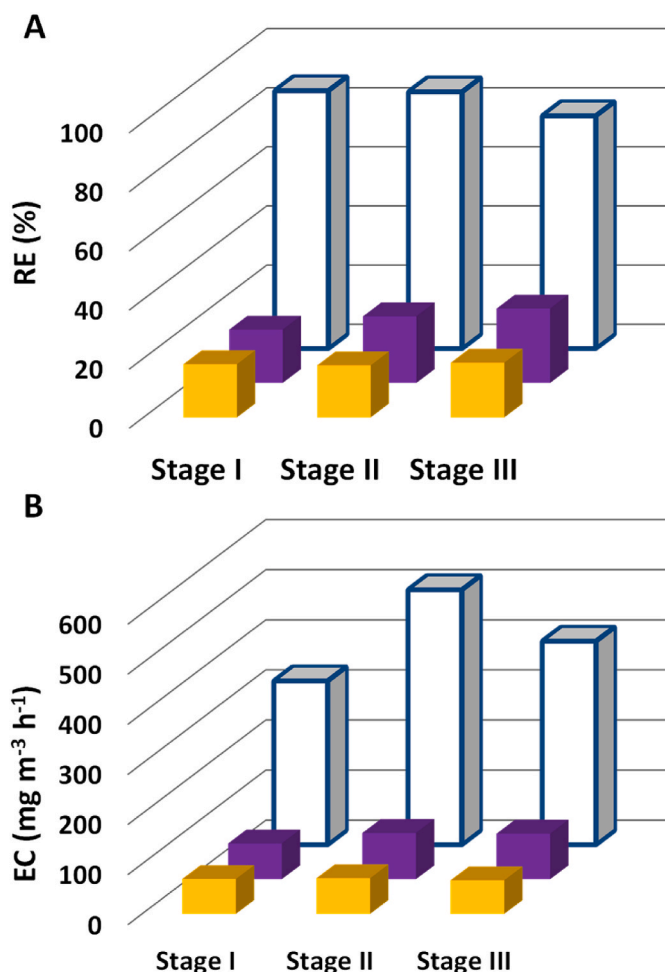


**Fig. 4.** Comparison of average VMS (A) removal efficiencies and (B) elimination capacities in the BTF-1 (yellow bars), BTF-2 (purple bars) and BTF-3 (white and blue bars) in the different stages of the test: EBRT of 60 min and TLV of 2 m h<sup>-1</sup> (Stage I), TLV increase to 4.5 m h<sup>-1</sup> in BTF-1 and 2 and EBRT decrease to 42 min in BTF-3 (Stage II), and addition of nanoparticles to the trickling solution (Stage III).

availability of both nutrients and electron acceptors.

### 3.3. Evolution of the CO<sub>2</sub> production

During the start-up of the experiment, CO<sub>2</sub> production gradually decreased in both BTF-1 and BTF-2 from initial values of 696 and 524 mg m<sup>-3</sup> h<sup>-1</sup> to average values of 276 ± 49 and 213 ± 57 mg m<sup>-3</sup> h<sup>-1</sup>, respectively, between days 15 and 56 (Fig. S4). The initial high CO<sub>2</sub> production was associated to cell debris resulting from the residual biomass that was not adsorbed onto the biofilm, followed by the subsequent degradation of the released TOC. On the contrary, the CO<sub>2</sub> productivity remained lower in BTF-3, with a gradual increase to 206 mg m<sup>-3</sup> h<sup>-1</sup> by day 25. From day 26 onwards, the average CO<sub>2</sub> production stabilized around 189 ± 38 mg m<sup>-3</sup> h<sup>-1</sup>. The differences in CO<sub>2</sub> production were likely linked to: (i) an initial adsorption of VMS on the activated carbon present in the packed bed of BTF-3, resulting in high VMS removals not associated with their biodegradation, (ii) the higher initial pH of the trickling solution in the BTF-3, which sequestered the CO<sub>2</sub> produced during VMS mineralization. In this sense, the pH in BTF-1 and BTF-2 remained relatively stable, with average values of 8.1 ± 0.2 and 7.8 ± 0.5. Conversely, in BTF-3, there was a progressive decrease in pH from 9.9 to 8.5 by the end of the experiment. It is noteworthy that a higher pH corresponds to higher CO<sub>2</sub> solubility in an aqueous solution.

By day 56, upon the BTFs reinoculation with the enriched culture, an increase in CO<sub>2</sub> production was observed in BTF-1, BTF-2 and BTF-3, reaching maximum values of 793, 938 and 831 mg m<sup>-3</sup> h<sup>-1</sup>, respectively. This overproduction aligned with the increase in VMS removal, thus indicating a correlation with the bacterial enrichment of the biofilm. This production fluctuated and finally decreased to 391, 376 and 434 mg m<sup>-3</sup> h<sup>-1</sup>, respectively, by the end of Stage I. At Stage II, when the trickling liquid velocity was raised to 4.5 m h<sup>-1</sup>, an initial CO<sub>2</sub> production increase to 620 and 894 was recorded in BTF-1 and BTF-2, respectively. However, these values immediately decreased stabilizing at 329 ± 74, 382 ± 122 and 310 ± 116 mg m<sup>-3</sup> h<sup>-1</sup> throughout the entire stage. In BTF-3, CO<sub>2</sub> production likewise rose to 714 mg m<sup>-3</sup> h<sup>-1</sup> as a result of the increased EC, stabilizing at 322 ± 120 mg m<sup>-3</sup> h<sup>-1</sup> for the rest of stage II. Similarly, CO<sub>2</sub> productions increased by day 112 when the NPs were added to the BTFs, reaching 1430, 1664 and 1048 mg m<sup>-3</sup> h<sup>-1</sup> in BTF-1, BTF-2 and BTF-3, respectively, to finally decrease below 300 mg m<sup>-3</sup> h<sup>-1</sup> at the end of the experiment. This increase could be linked to the potential release of organic substances inherent to the NPs manufacturing process (Fullana Font and Calderón Roca, 2022), which were subsequently mineralized within the biofilm.

### 3.4. Characterization of the liquid trickling solution

In the liquid trickling solution both nitrate and total nitrogen remained constant in BTF-1 and 2 at values ranging from 320 to 370 mg L<sup>-1</sup> until day 105, when a slight decrease was recorded (Fig. S5). On the contrary, low initial nitrate and total nitrogen values of 232 and 211 mg L<sup>-1</sup> were recorded in BTF-3, likely due to the adsorption of nitrate on the AC and the higher microbial activity compared with BTFs 1 and 2. These values progressively increased and stabilized at 347 ± 11 and 388 ± 24 mg L<sup>-1</sup> for TN and nitrate concentrations, respectively, by day 77. This increase coincided with the reduction in the system's performance throughout the experiment, particularly noticeable for L2, suggesting a correlation between nitrogen consumption by microorganisms and the decline in performance.

The TOC concentration progressively decreased from initial values of 34, 54, and 27 mg L<sup>-1</sup> to average values of 14 ± 4, 18 ± 3, and 6 ± 3 mg L<sup>-1</sup> (between days 70 and 105) in the trickling solution of BTF-1, BTF-2, and BTF-3, respectively (Fig. S6). The TOC concentration in BTF-3 remained constant until the end of the experiment. However, an increase in the TOC concentration to 59 and 69 mg L<sup>-1</sup> was observed in BTF-1 and BTF-2, associated to the organic substance released from nanoparticles, subsequently decreasing along Stage III as it was mineralized. In BTF-3, the organic substances were likely absorbed in the activated carbon and directly mineralized in the biofilm, as evidenced by the absence of TOC increase during Stage III.

Finally, the IC concentration remained at average values of 9 ± 3 and 8 ± 2 mg L<sup>-1</sup> in the trickling solution of BTF-1 and BTF-2 (Fig. S6). However, the IC concentration initially increased in BTF-3, reaching 73 mg L<sup>-1</sup> by day 21. Afterwards, the concentration progressively decreased to an average value of 19 ± 3 mg L<sup>-1</sup>. The higher IC concentration of BTF-3 compared to BTF-1 and BTF-2 was attributed to the higher initial CO<sub>2</sub> absorption in the trickling liquid solution and the progressive decrease along with the pH.

Based on the observed trends in nitrate, TOC, and IC concentrations in the trickling liquid solutions, BTF-3 exhibited higher nitrogen consumption and more effective overall organic carbon mineralization. These findings demonstrate the impact of activated carbon in the regulation of nutrient and carbon dynamics.

### 3.5. Bacterial community

According to the bacterial diversity analysis from the metagenomic data, the bacterial communities present in BTF-1 and BTF-2 were considerably similar by the end of operation. However, BTF-3 exhibited significantly more diverse communities. BTF-1 and BTF-2 had a higher

percentage of shared bacterial species (more than 35%), indicating similarities in their bacterial compositions (Fig. S7). In contrast, BTF-3 shared a lower percentage (14% and 12%) of species with BTF-1 and BTF-2, respectively. This implies that the community of BTF-3 diversified along time, having a distinct bacterial community composition compared to the other BTFs. The dominant genus in BTF-1 was *Corynebacterium* with a relative abundance of 35.6%, followed by *Thiobacillus* and *Acetobacterium* with abundances of 10.0 and 8.4%. In BTF-2, *Thermomonas* (23.3%) and *Thiobacillus* (18.3%) were the most representative genera followed by other less abundant bacteria of the genera *Leptolinea* (8.2%), *Clostridium* (7.9%), *Limnobacter* (6.7%), *Denitratisoma* (6.7%), *Thauera* (6.4%) and *Acetobacterium* (6.2%). Finally, *Thiobacillus* (26.2%) and *Aquimonas* (11.9%) were the most representative genera at the end of the operation of BTF-3, followed by *Thauera* (8.4%), *Clostridium* (6.7%), *Lactobacillus* (5.7%) and *Mycobacterium* (5.5%).

Among these bacterial communities, *Parvibaculum* was the only one previously identified as being involved in VMS biofiltration under anoxic conditions (Pascual et al., 2022b). The genus *Thiobacillus* was among the most representative bacteria in all the bioreactors (Fig. 5 and Fig. S8). It represents a sulphur-oxidizing genus of bacteria primarily dedicated to the removal of hydrogen sulphide from gas streams (Syed et al., 2006). For instance, *Thiobacillus thioparus* has been investigated for the removal of H<sub>2</sub>S from a waste air stream in a BTF packed with polyurethane foam (Ramírez et al., 2009). Other species within this genus have been identified as bacteria involved in Fe(II) oxidation and nitrate reduction (*Thiobacillus denitrificans*) (Liu et al., 2019). The dominance of *Thiobacillus* in the reactors might be attributed to the high nitrate concentration present in all the BTFs, which could have served as electron acceptor.

The other dominant genera, such as *Thermomonas*, *Corynebacterium*, *Aquimonas* and *Thauera* have been identified as versatile bacteria associated with the degradation of VOCs and complex organic compounds, which indicated their likely involvement in the removal of VMS. *Thermomonas* bacterial members are related to heterotrophic denitrification under different organic sources in wastewater treatment plants (Xing et al., 2018). *Corynebacterium* was classified as a VOC degrading anaerobic bacterium for several VOCs, such as trichloroethane and styrene (Li et al., 2020; Malhautier Nadia Khammar Sandrine Bayle Jean-Louis Fanlo, 2005), and complex organic compounds, such as

*n*-alkanes (Zhang et al., 2016). In the case of *Aquimonas*, previous research has identified this genus as potential degraders of styrene in a BTF packed with polypropylene rings, with their abundance increasing with the styrene load (Portune et al., 2020). *Aquimonas* was also detected among the dominant genera in a toluene degrading community (Wei et al., 2019). Moreover, certain species of denitrifying bacteria within the genus *Thauera* have demonstrated the ability to grow on various VOCs such as toluene, ethylbenzene, chlorobenzene, acetone, isopropyl alcohol, ethyl acetate, *n*-hexane and tetrahydrofuran (Lu et al., 2018; Shinoda et al., 2004).

These results indicated that a consortium composed of the different genera was responsible for the degradation of siloxanes in the BTFs. The diversification observed in BTF-3, along with the minor differentiation in its bacterial composition compared to BTF-1 and BTF-2, was likely correlated with the superior performance on VMS removal and the advantageous conditions facilitated by the packing material of BTF-3 for bacterial growth. Specifically, the porous structure of activated carbon could facilitate the direct interspecies electron transfer among the diverse microorganisms involved in VMS degradation pathways. This mechanism not only plays a crucial role in microbial interactions within anaerobic environments but may also explain the greater microbial diversity observed in BTF-3, as DIET promotes complex and cooperative interactions among different species (Bonaglia et al., 2020). It is noteworthy to highlight that, except for the genus *Parvibaculum*, the other identified genera had not been previously associated with siloxane degradation. Therefore, the obtained results pave the way for further research to elucidate the specific role of each genus in this process.

#### 4. Conclusions

This research revealed the significant role of activated carbon on siloxanes biofiltration. The BTF packed with a mix of activated carbon and Kaldnes rings (20:80 v/v) achieved total VMS removals of up to 90%, with complete removal of L3 and D4. Lower REs were obtained for L2, attributed to the activated carbon's preference for VMS with higher molecular weight and critical diameter (L3, D4, D5), that overshoots the adsorption of smaller VMS (L2). In contrast, BTFs with Kaldnes rings and polyurethane foam showed lower removals, peaking at around 40%. The superior performance of BTF-3 confirmed the benefits of activated

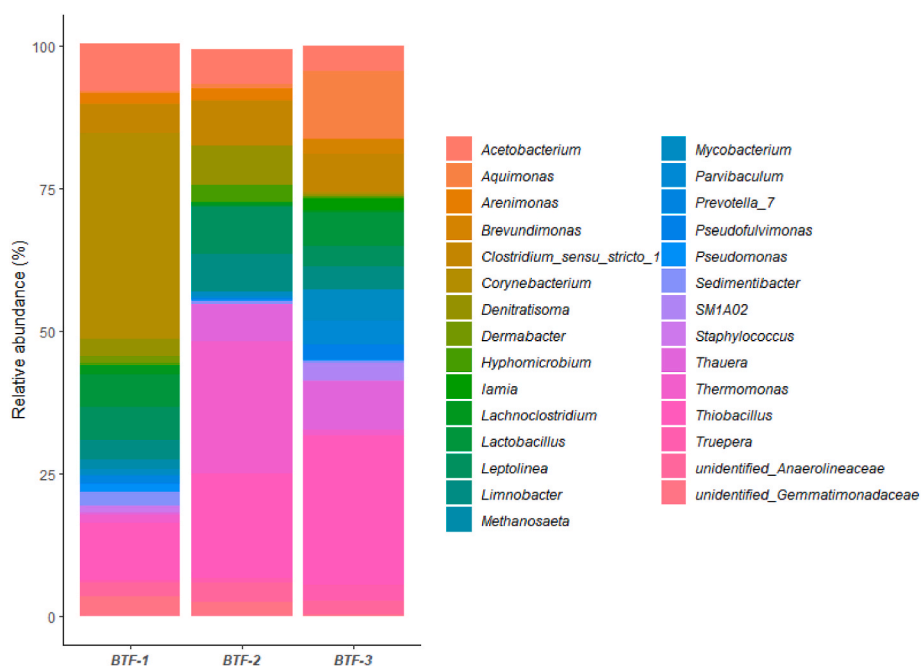


Fig. 5. Bar plot of the community structure (relative abundance) at genus level in BTF-1, BTF-2 and BTF-3 at the end of the experiment.



carbon as a packing material, promoting efficient biomass growth and mitigating mass transfer limitations through its adsorption capacity. The increasing in the trickling liquid velocity from 2 to 4.5 m h<sup>-1</sup> in BTF-1 and BTF-2, as well as the addition of Fe-carbon nanoparticles to the three BTFs did not significantly improve performance. The operating conditions in BTF-3 were optimized by reducing the EBRT from 60 to 42, which sustained a total VMS REs of ~87% while increasing EC from 366 to 509 mg m<sup>-3</sup> h<sup>-1</sup>. Finally, the bacterial community analysis revealed new genera not previously associated with VMS removal, such as *Thermomonas*, *Corynebacterium*, *Aquimonas* and *Thauera*, with *Parvibaculum* being the dominant genera during anaerobic VMS-biodegradation. Overall, this study significantly contributes to the optimization of siloxane biofiltration by highlighting the importance of the chosen packing material on mass transfer and biomass growth efficiency and identifying new bacterial genera as potential microorganisms for VMS degradation.

### CRedit authorship contribution statement

**Celia Pascual:** Writing – original draft, Visualization, Supervision, Methodology, Formal analysis, Conceptualization. **David Antolín:** Investigation, Data curation. **Sara Cantera:** Writing – review & editing, Visualization, Methodology. **Raúl Muñoz:** Writing – review & editing, Resources, Funding acquisition. **Raquel Lebrero:** Writing – review & editing, Supervision, Resources, Project administration, Methodology, Funding acquisition, Conceptualization.

### Declaration of competing interest

The authors declare that they have no known competing financial interests or personal relationships that could have appeared to influence the work reported in this paper.

### Acknowledgements

This work was supported by the URBIOFIN project. The project has received funding from the Bio Based Industries Joint Undertaking under the European Union's Horizon 2020 research and innovation program under grant agreement No 745785. The support from the regional government of Castilla y León and the EU-FEDER programme (CLU 2017–09, CL-EI-2021-07 and UIC 315) is also acknowledged. The European Commission-H2020- MSCA-IF-2019 is also gratefully acknowledged for the financial support of the project ENHANCEMENT (897284).

### Appendix A. Supplementary data

Supplementary data to this article can be found online at <https://doi.org/10.1016/j.jenvman.2024.122862>.

### Data availability

Data will be made available on request.

### References

- Accettola, F., Guebitz, G.M., Schoefner, R., 2008. Siloxane removal from biogas by biofiltration: biodegradation studies. *Clean Technol. Environ. Policy* 10, 211–218. <https://doi.org/10.1007/s10098-007-0141-4>.
- Alton, M.W., Browne, E.C., 2021. Atmospheric degradation of cyclic volatile methyl siloxanes: radical chemistry and oxidation products. *ACS Environmental Au* 2, 263–274. <https://doi.org/10.1021/ACSENVIRONAU.1C00043/ASSET/IMAGES/LARGE/VG1C00043.0006.JPEG>.
- Alves, C.M.A.C., Abreu, F.O.M.S., Araújo, R.S., Oliveira, M.L.M., 2023. Recent advances in siloxanes removal from biogas and their efficiency: a short review. *Chem. Pap.* <https://doi.org/10.1007/s11696-022-02460-1>.
- Bonaglia, S., Broman, E., Brindefalk, B., Hedlund, E., Hjorth, T., Rolff, C., Nascimento, F. J.A., Udekwi, K., Gunnarsson, J.S., 2020. Activated carbon stimulates microbial diversity and PAH biodegradation under anaerobic conditions in oil-polluted

- sediments. *Chemosphere* 248. <https://doi.org/10.1016/j.chemosphere.2020.126023>.
- Bu, H., Carvalho, G., Yuan, Z., Bond, P., Jiang, G., 2021. Biotrickling filter for the removal of volatile sulfur compounds from sewers: a review. *Chemosphere* 277, 130333. <https://doi.org/10.1016/j.chemosphere.2021.130333>.
- de Arespacochaga, N., Raich-Montiu, J., Crest, M., Cortina, J.L., 2020. Presence of siloxanes in sewage biogas and their impact on its energetic valorization. *Handb. Environ. Chem.* 89, 131–157. <https://doi.org/10.1007/978-2018-372/COVER>.
- Duan, H., Koe, L.C.C., Yan, R., 2005. Treatment of H<sub>2</sub>S using a horizontal biotrickling filter based on biological activated carbon: reactor setup and performance evaluation. *Appl. Microbiol. Biotechnol.* 67. <https://doi.org/10.1007/s00253-004-1771-7>.
- Duan, H., Koe, L.C.C., Yan, R., Chen, X., 2006. Biological treatment of H<sub>2</sub>S using pellet activated carbon as a carrier of microorganisms in a biofilter. *Water Res.* 40. <https://doi.org/10.1016/j.watres.2006.05.021>.
- Edgar, R.C., Haas, B.J., Clemente, J.C., Quince, C., Knight, R., 2011. UCHIME improves sensitivity and speed of chimera detection. *Bioinformatics* 27. <https://doi.org/10.1093/bioinformatics/btr381>.
- Estrada, J.M., Lebrero, R., Quijano, G., Pérez, R., Figueroa-González, I., García-Encina, P. A., Muñoz, R., 2014. Methane abatement in a gas-recycling biotrickling filter: evaluating innovative operational strategies to overcome mass transfer limitations. *Chem. Eng. J.* 253, 385–393. <https://doi.org/10.1016/j.cej.2014.05.053>.
- Fullana Font, A., Calderón Roca, B., 2022. WO2022023596 - METHOD FOR OBTAINING ZEROVALENT IRON NANOPARTICLES.
- Gaj, K., 2020. Adsorptive biogas purification from siloxanes—a critical review. *Energies* 2020 13. <https://doi.org/10.3390/EN13102605>, 2605 13, 2605.
- Kluytmans, J.H.J., van Wachem, B.G.M., Kuster, B.F.M., Schouten, J.C., 2003. Mass transfer in sparged and stirred reactors: influence of carbon particles and electrolyte. *Chem. Eng. Sci.* 58. <https://doi.org/10.1016/j.ces.2003.05.004>.
- Korotta-gamage, S.M., Sathasivan, A., 2017. *Chemosphere A Review: Potential and Challenges of Biologically Activated Carbon to Remove Natural Organic Matter in Drinking Water Puri Fi Cation Process*, vol. 167, pp. 120–138. <https://doi.org/10.1016/j.chemosphere.2016.09.097>.
- Lebrero, R., Gondim, A.C., Pérez, R., García-Encina, P.A., Muñoz, R., 2014. Comparative assessment of a biofilter, a biotrickling filter and a hollow fiber membrane bioreactor for odor treatment in wastewater treatment plants. *Water Res.* 49. <https://doi.org/10.1016/j.watres.2013.09.055>.
- Li, T., Li, H., Li, C., 2020. A review and perspective of recent research in biological treatment applied in removal of chlorinated volatile organic compounds from waste air. <https://doi.org/10.1016/j.chemosphere.2020.126338>.
- Li, Y., Zhang, W., Xu, J., 2014. Siloxanes removal from biogas by a lab-scale biotrickling filter inoculated with *Pseudomonas aeruginosa* S240. *J. Hazard Mater.* 275, 175–184. <https://doi.org/10.1016/j.jhazmat.2014.05.008>.
- Liu, T., Chen, D., Li, X., Li, F., 2019. Microbially mediated coupling of nitrate reduction and Fe(II) oxidation under anoxic conditions. *FEMS Microbiol. Ecol.* <https://doi.org/10.1093/femsec/fiz030>.
- Lu, L., Wang, G., Yeung, M., Xi, J., Hu, H.Y., 2018. Response of microbial community structure and metabolic profile to shifts of inlet VOCs in a gas-phase biofilter. *Amb. Express* 8. <https://doi.org/10.1186/s13568-018-0687-z>.
- Lv, S., Hou, X., Zheng, Y., Ma, Z., 2023a. Hexamethyldisiloxane removal from biogas using a Fe<sub>3</sub>O<sub>4</sub>-urea-modified three-dimensional graphene aerogel. *Molecules* 28. <https://doi.org/10.3390/molecules28186622>.
- Lv, S., Wang, Y., Zheng, Y., Ma, Z., 2023b. Removal of hexamethyldisiloxane via a novel hydrophobic (3-Aminopropyl)Trimethoxysilane-modified activated porous carbon. *Molecules* 28. <https://doi.org/10.3390/molecules28186493>.
- Magoč, T., Salzberg, S.L., 2011. FLASH: fast length adjustment of short reads to improve genome assemblies. *Bioinformatics*. <https://doi.org/10.1093/bioinformatics/btr507>.
- Malhautier Nadia Khammar Sandrine Bayle Jean-Louis Fanlo, L., 2005. MINI-REVIEW Biofiltration of volatile organic compounds. *Appl. Microbiol. Biotechnol.* 68, 16–22. <https://doi.org/10.1007/s00253-005-1960-z>.
- Pascual, C., Cantera, S., Lebrero, R., 2021a. Volatile siloxanes emissions: impact and perspectives. *Trends Biotechnol.* 39, 1245–1248. <https://doi.org/10.1016/j.tibtech.2021.05.003>.
- Pascual, C., Cantera, S., Muñoz, R., Lebrero, R., 2023. Assessment of the mass transfer strategy and the role of the active bacterial population on the biological degradation of siloxanes. *Fuel* 350. <https://doi.org/10.1016/j.fuel.2023.128851>.
- Pascual, C., Cantera, S., Muñoz, R., Lebrero, R., 2022a. Innovative polishing stage in biogas upgrading: siloxanes abatement in an anoxic two-phase partitioning biotrickling filter. *J. Clean. Prod.* 371. <https://doi.org/10.1016/j.jclepro.2022.133427>.
- Pascual, C., Cantera, S., Muñoz, R., Lebrero, R., 2022b. Innovative polishing stage in biogas upgrading: siloxanes abatement in an anoxic two-phase partitioning biotrickling filter Anoxic biotrickling filter Biogas upgrading Silicone oil Siloxanes Two-phase partitioning bioreactor. *J. Clean. Prod.* 371, 133427. <https://doi.org/10.1016/j.jclepro.2022.133427>.
- Pascual, C., Cantera, S., Muñoz, R., Lebrero, R., 2021b. Siloxanes removal in a two-phase partitioning biotrickling filter: influence of the EBRT and the organic phase. *Renew. Energy* 177. <https://doi.org/10.1016/j.renene.2021.05.144>.
- Pascual, C., Cantera, S., Muñoz, R., Lebrero, R., 2020. Comparative assessment of two biotrickling filters for siloxanes removal: effect of the addition of an organic phase. *Chemosphere* 251, 126359. <https://doi.org/10.1016/j.chemosphere.2020.126359>.
- Pérez, M.C., Alvarez-Hornos, F.J., Engesser, K.H., Dobslaw, D., Gabaldón, C., 2016. Removal of 2-butoxyethanol gaseous emissions by biotrickling filtration packed with polyurethane foam. *N Biotechnol* 33, 263–272. <https://doi.org/10.1016/j.NBT.2015.11.006>.

- Popat, S.C., Deshusses, M.A., 2008. Biological removal of siloxanes from landfill and digester gases: opportunities and challenges. *Environ. Sci. Technol.* 42, 8510–8515. <https://doi.org/10.1021/es801320w>.
- Portune, K.J., Carmen P Erez, M., Alvarez-Hornos, J., Gabald, C., 2020. Contribution of bacterial biodiversity on the operational performance of a styrene biotrickling filter. <https://doi.org/10.1016/j.chemosphere.2019.125800>.
- Quast, C., Pruesse, E., Yilmaz, P., Gerken, J., Schweer, T., Yarza, P., Peplies, J., Glöckner, F.O., 2013. The SILVA ribosomal RNA gene database project: improved data processing and web-based tools. *Nucleic Acids Res.* <https://doi.org/10.1093/nar/gks1219>.
- Ramírez, M., Gómez, J.M., Aroca, G., Cantero, D., 2009. Removal of hydrogen sulfide by immobilized *Thiobacillus thiooparus* in a biotrickling filter packed with polyurethane foam. *Bioresour. Technol.* 100. <https://doi.org/10.1016/j.biortech.2009.05.022>.
- Rivera-Montenegro, L., Valenzuela, E.I., González-Sánchez, A., Muñoz, R., Quijano, G., 2023. Volatile methyl siloxanes as key biogas pollutants: occurrence, impacts and treatment technologies. *Bioenergy Res.* <https://doi.org/10.1007/s12155-022-10525-y>.
- Rybarczyk, P., Szulczyński, B., Gębicki, J., Hupka, J., 2019. Treatment of malodorous air in biotrickling filters: a review. *Biochem. Eng. J.* <https://doi.org/10.1016/j.bej.2018.10.014>.
- Sakhaei, A., Zamir, S.M., Rene, E.R., Veiga, M.C., Kennes, C., 2023. Neural network-based performance assessment of one- and two-liquid phase biotrickling filters for the removal of a waste-gas mixture containing methanol,  $\alpha$ -pinene, and hydrogen sulfide. *Environ. Res.* 237. <https://doi.org/10.1016/j.envres.2023.116978>.
- Santos-Clotas, E., Cabrera-Codony, A., Boada, E., Gich, F., Muñoz, R., Martín, M.J., 2019a. Efficient removal of siloxanes and volatile organic compounds from sewage biogas by an anoxic biotrickling filter supplemented with activated carbon. *Bioresour. Technol.* 294, 122136. <https://doi.org/10.1016/j.biortech.2019.122136>.
- Santos-Clotas, E., Cabrera-Codony, A., Ruiz, B., Fuente, E., Martín, M.J., 2019b. Sewage biogas efficient purification by means of lignocellulosic waste-based activated carbons. *Bioresour. Technol.* 275, 207–215. <https://doi.org/10.1016/j.biortech.2018.12.060>.
- Shen, M., Zhang, Y., Hu, D., Fan, J., Zeng, G., 2018. A review on removal of siloxanes from biogas: with a special focus on volatile methylsiloxanes. *Environ. Sci. Pollut. Control Ser.* 25, 30847–30862. <https://doi.org/10.1007/s11356-018-3000-4>.
- Shinoda, Y., Sakai, Y., Uenishi, H., Uchihashi, Y., Hiraishi, A., Yukawa, H., Yurimoto, H., Kato, N., 2004. Aerobic and anaerobic toluene degradation by a newly isolated denitrifying bacterium, *Thauera* sp. strain DNT-1. *Appl. Environ. Microbiol.* 70. <https://doi.org/10.1128/AEM.70.3.1385-1392.2004>.
- Standardization, 2018. EN 16723-2:2018. Natural Gas and Biomethane for Use in Transport and Biomethane for Injection in the Natural Gas Network.
- Sun, D., Li, J., An, T., Xu, M., Sun, G., Guo, J., 2012. Bacterial community diversity and functional gene abundance of structured mixed packing and inert packing materials based biotrickling filters. *Biotechnol. Bioproc. Eng.* 17. <https://doi.org/10.1007/s12257-011-0239-8>.
- Syed, M., Soreanu, G., Falletta, P., Béland, M., 2006. Removal of Hydrogen Sulfide from Gas Streams Using Biological Processes - A Review. *Canadian Biosystems Engineering/Le Genie des biosystems au Canada*.
- Tran, V.T.L., Gélín, P., Ferronato, C., Chovelon, J.M., Fine, L., Postole, G., 2019. Adsorption of linear and cyclic siloxanes on activated carbons for biogas purification: sorbents regenerability. *Chem. Eng. J.* 378, 122152. <https://doi.org/10.1016/j.cej.2019.122152>.
- Urban, W., Lohmann, H., Gómez, J.I.S., 2009. Catalytically upgraded landfill gas as a cost-effective alternative for fuel cells. *J. Power Sources* 193, 359–366. <https://doi.org/10.1016/j.jpowsour.2008.12.029>.
- Urbaniec, K., Kasperczyk, D., Thomas, M., 2020. Biofilters versus bioscrubbers and biotrickling filters : state-of-the-art biological air treatment 29–51. <https://doi.org/10.1016/B978-0-12-819064-7.00002-9>.
- Vargas-Estrada, L., Hoyos, E.G., Sebastian, P.J., Muñoz, R., 2023. Influence of mesoporous iron based nanoparticles on *Chlorella sorokiniana* metabolism during photosynthetic biogas upgrading. *Fuel* 333. <https://doi.org/10.1016/j.fuel.2022.126362>.
- Wei, Z.S., He, Y.M., Huang, Z.S., Xiao, X.L., Li, B.L., Ming, S., Cheng, X.L., 2019. Photocatalytic membrane combined with biodegradation for toluene oxidation. <https://doi.org/10.1016/j.ecoenv.2019.109618>.
- Wickham, H., 2009. ggplot2, Ggplot2. Springer, New York. <https://doi.org/10.1007/978-0-387-98141-3>.
- Xing, W., Li, J., Li, P., Wang, C., Cao, Y., Li, D., Yang, Y., Zhou, J., Zuo, J., 2018. Effects of residual organics in municipal wastewater on hydrogenotrophic denitrifying microbial communities. *Journal of Environmental Sciences* 65, 262–270. <https://doi.org/10.1016/J.JES.2017.03.001>.
- Zhang, H., Tang, J., Wang, L., Liu, J., Gajanan Gurav, R., Sun, K., 2016. A novel bioremediation strategy for petroleum hydrocarbon pollutants using salt tolerant *Corynebacterium variabile* HRJ4 and biochar. <https://doi.org/10.1016/j.jes.2015.12.023>.